

## AUTOMATIC REGISTRATION OF SAR AND OPTICAL IMAGE BASED ON LINE AND GRAPH SPECTRAL THEORY

Jun Zhao<sup>1,\*</sup>, Shuxin Gao<sup>1</sup>, Haigang Sui<sup>2</sup>, Yulin Li<sup>1</sup>, Lan Li<sup>3</sup>

<sup>1</sup> Shandong Provincial Institute of Land Surveying and Mapping, Jinan,  
250013, P. R. China, hebeizhaojun@163.com

<sup>2</sup> State Key Laboratory of Information Engineering in Surveying, Wuhan University, Wuhan,  
430079, P. R. China, haigang\_sui@263.net

<sup>3</sup> Institute of Forest Resources Information Technique, Chinese Academy of Forestry, Beijing,  
100091, P. R. China, lilanlan1128@163.com

**KEY WORDS:** SAR image, optical image, image registration, Spectral Graph Theory, Voronoi diagram

### ABSTRACT:

In this paper, a novel registration method is proposed by integrating the graph spectral theory and line features. The principal steps of our algorithm are as follows. Firstly, the images are filtered to enhance the reliability and robustness of registration, and line features are acquired by Hough Transform. Secondly, the original point features can be obtained by calculating the line intersections. The points are normalized to reduce computational complexity. Thirdly, voronoi diagrams of two point sets are extracted respectively. The original corresponding point sets are determined by corresponding voronoi diagrams, which can be obtained by Graph Spectral Theory. At last, RANSAC is used to remove the wrong corresponding points. The transform relationship of the two input images can be achieved using the corresponding point sets. The experimental results show that the proposed method can achieve high accuracy for the registration between optical and SAR images.

### 1. INTRODUCTION

With the development of remote sensing technique, there is an increasing interest on images from different sensors. Image registration is the fundamental pre-processing to remote sensing application, which has been widely used in different fields such as target identification, surface reconstruction, multi-resource data fusion, and change detection. However, because of the different imaging mechanisms between multi-source images, automatic registration becomes a big challenge, especially between SAR and optical images. The speckle noise makes it difficult to extract accurate corresponding features between SAR and optical images. In this paper, a novel registration method is proposed by integrating graph spectral theory with line features.

Present image registration techniques broadly fall into two types: area-based and feature-based techniques. In the area-based method, techniques based on mutual information have been proposed for SAR and optical image registration. However, the absence of local spatial information in mutual information reduces the robustness of the techniques. To overcome this drawback, improvements have been proposed, such as combining mutual information with orientation information (Shu *et al.* 2005) or image gradient (Wang *et al.* 2005). Suri and

Reinartz (2008) improved histogram bin size utilizing B-spline kernels, then used mutual information to register SAR and optical images. However, due to the different target reflection characteristic and speckle noise, the area-based measure often leads to unreliable results. What's more, most of the area-based methods can achieve high accuracy only for images with small misalignment. In contrast, feature-based techniques are more suitable for the problem.

Many different methods based on common features have been proposed to solve the problem of automatically registering of SAR and Optical images. These features usually include point features, linear features (edge, road, river) and area features. Wu (2011) proposed a novel method based on SIFT and CRA similarity measure, and obtained accurate parameters using Quadratic polynomial and RANSAC algorithm. However, it is difficult to directly exact corresponding point features because of speckle noise. Improvements have been made to overcome the setback. In some methods, binary images or outline images were extracted, then common point features were utilized to register images (Li *et al.* 1993, Li *et al.* 1995, Peng 2009). Zhang *et al.* (2007) used the centers of closed surface features as the match points. Jia and Zhang(2009) first exacted edge maps, then got patches using mean sift segmentation algorithm in both images as common features to register SAR and optical

\* Corresponding author: Zhao Jun, graduated from the Wuhan University. Major in image processing and application of remote sensing. E-mail: hebeizhaojun@163.com.

images. Recently, sophisticated approaches have been developed based on multi-features or multi-layer feature (Dare and Ian 2001, Zhang *et al.* 2004, Wang *et al.* 2010). However, only when the precision of edge detection was high, could the above methods have good performance. Besides, the closed area features cannot be exacted in all of images. To solve it, the method based on line and graph spectral theory was proposed to register SAR and optical image.

The principal steps of our algorithm are as follows. Firstly, the images are filtered to enhance the reliability and robustness of registration. And line features are acquired by Hough Transform (Kesidis and Papamarkos 2000). Secondly, the original point features can be obtained by calculating the line intersections. The points are normalized to reduce computational complexity. Thirdly, voronoi diagrams of two point sets are extracted respectively. The original corresponding point sets are determined by corresponding voronoi diagrams, which can be obtained by using Graph Spectral Theory (Longuet-Higgins and Scott 1991; Shapiro and Brady 1992). At last, RANSAC (Fischler and Bolles 1987) is used to remove the wrong corresponding points. The transform relationship of the two input images can be achieved using the corresponding point sets. Compared with traditional registration methods, the proposed offers several advantages. On the one hand, the proposed method considers both global information and local geometric information of the images to improve the accuracy of corresponding features. On the other hand, computational complexity is reduced significantly, because the graph spectral can effectively avoid combinatorial or iterative.

The remainder of this paper is presented as follows. In Section 2, our method is formulated and applied to the registration between SAR and optical images. Some experimental results are given in Section 3, before we conclude the paper in Section 4.

## 2. METHODOLOGY

The basic principle of the proposed method is outlined in Fig. 1.

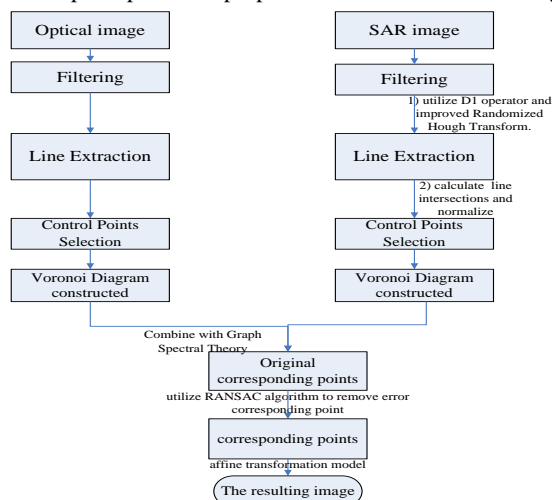


Fig. 1 Algorithm flowchart

### 2.1 Linear features extraction and control points selection

1) Edge detection: Edge is one of the most basic features of an image. At present, a variety of edge detection methods have been introduced, such as the Prewitt operator, Sobel operator, Laplacian operator, Robert operator and Canny operator. Among all these methods, the Canny operator, which can propose an appropriate optimality criterion and provide desirable result, is selected for edge extraction in the paper. Thus, in the method, Canny operator is utilized to exact edge feature of optical images. However, due to different imaging mechanisms between optical and SAR images, D1 (Touzi *et al.* 1988 ) is used to exact edge feature of SAR images.

2) Line features extraction. Extracting line features with high accuracy, it is critical to obtain satisfying result. Among all these methods, the main advantage of the Hough transform technique is that it is tolerant of gaps in feature boundary descriptions and is relatively unaffected by image noise. Meanwhile, as classical approach for line detection, the Hough Transform is still widely used to identify positions of parameterized shapes. In the paper, Hough Transform is utilized to extract line features from images.

3) Control points selection. After line features extraction, line intersections can be obtained as the original point features. It is necessary to normalize point sets to reduce the number of parameters and improve the computing speed. Thus, affine transformation of two point sets can be converted to simple rotation transformation.

### 2.2 Voronoi diagram

Voronoi diagram differs from other areas of computational geometry and its origin can be traced back to Descartes in the 17th century. In mathematics, a voronoi diagram is a way to divide space into a number of regions. A set of points (called sites, seeds, or generators) is specified beforehand and for each seed there will be a corresponding region consisting of all points closer to that seed than to others. It is dual to the Delaunay triangulation.

The distinct advantages of Voronoi diagram facilitate the utilization of local geometric information.

a) In a Euclidean space with point sets, as the dual graph of the Delaunay triangulation, the voronoi diagram of point sets is more stable.

b) Compared to common polygon, the similarity criterion of voronoi polygon is more rigorous. It meets the similarity of polygon shape, as well as, the position correspondence of point contained.

c) If some points are inserted or removed, the change remains the local diagram and does not affect global stability, as shown in Fig. 2.

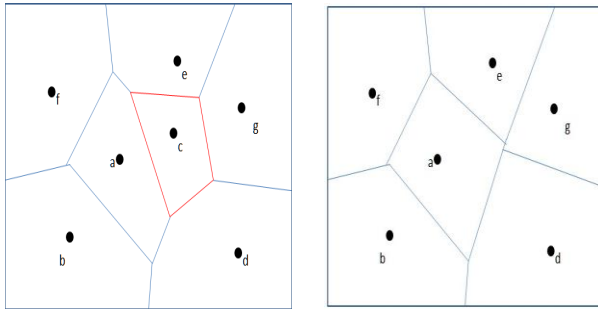


Fig.2

d) If point p and the polygon generating from p are known, other points around point p can be found.

e) After affine translation, voronoi cells have some stable property. Changes caused by affine translation or distortion, may change the shape of the voronoi cells, however, the global topological relationship cannot be affected.

From the above analysis, we can conclude that voronoi diagram feature is more stable and suitable to represent local geometric information of line intersections. Extracting voronoi diagrams of control points as registration element, makes the method not sensitive to noise or outliers, and enhances the reliability and robustness of registration.

### 2.3 The improved method

In the traditional Spectral Graph Theory, Gaussian-weighted adjacency matrix for two points is constructed, then the transform parameters can be acquired by performing singular value decomposition on the above matrices. However, the result is not desirable when the transformation parameters are large. The improved method contains the following steps:

- 1) Voronoi diagrams are generated from two control point sets, which can be obtained by the technique mentioned in 2.1.
- 2) A Gaussian-weighted proximity matrix H can be created, recording the distances between voronoi polygons from the two images.

$$H_{ij} = e^{-\frac{d_{ij}^2}{2\sigma^2}} \quad (i=1 \dots m, j=1 \dots n) \quad (1)$$

where  $i, j$  = voronoi polygon constructed from different point sets  
 $\sigma$  =constant based on interaction between features  
 $d_{ij}$  =the distance between i and j

- 3) Perform the singular value decomposition (SVD) of G

$$G = TDU^T \quad (2)$$

where D =the diagonal matrix containing the (positive) singular values along its diagonal elements in descending numerical order,  
 U, T = orthogonal matrix

- 4) Replace every diagonal element of D with 1, thus matrix D can be converted to a new matrix E, and then compute the product

$$P = TEU^T \quad (3)$$

This new matrix P amplifies good pairings and attenuates bad ones, as well as, has the same shape as the proximity matrix G. Thus, if  $P_{ij}$  is both the greatest element in its row and column, then the two voronoi polygons are regarded corresponding.

At last, RANSAC is used to remove the wrong corresponding points and improve registration accuracy. The transform relationship of the two input images can be achieved using the corresponding point sets.

### 3. EXPERIMENTAL RESULTS

Experiments were performed on three pairs of images with various resolutions of different areas. We illustrate the effectiveness of the proposed method by comparing the performance with the MIOI algorithm (Shu 2005) using airport images, overpass images and port images.

- (1) Fig. 1 shows the optical and SAR images acquired around an airport and the registration results. The optical image with 6.5m resolution and SAR image with 5m resolution are shown in Fig.1 (a) and Fig.1 (b) respectively. The registration result of the proposed method is shown in Fig.1 (c). The result of MIOI is shown in Fig.1 (d).



(a)



(b)



(c)



(d)

Fig.1 Registration of optical and SAR images.

(a) Optical image (b) SAR image

(c) The result of the proposed method. (d) The result of MIOI.

(2) Fig.2 shows the optical and SAR images acquired around a port and the registration results. The optical image and SAR image are shown in Fig.2 (a) and Fig.2 (b) respectively. The registration result of the proposed method is shown in Fig.2 (c). The result of MIOI is shown in Fig. 2(d).



(a)



(b)



(c)



(d)

Fig.2 Registration of optical and SAR images.

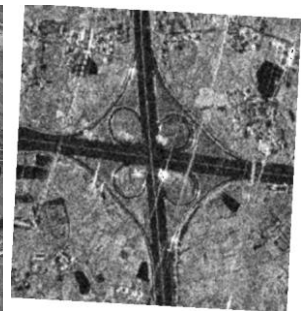
(a) Optical image (b) SAR image

(c) The result of the proposed method. (d) The result of MIOI.

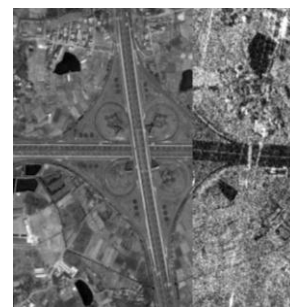
(3) Fig.3 shows the optical and SAR images acquired around an overpass and the registration results. The optical image obtained from Google Earth and Cosmo image with 1m resolution are shown in Fig.3 (a) and Fig.3 (b) respectively. The registration result of the proposed method is shown in Fig.3 (c). The result of MIOI is shown in Fig.3 (d).



(a)



(b)



(c)



(d)

Fig.3 Registration of optical and SAR images.

(a) Optical image (b) SAR image

(c) The result of the proposed method. (d) The result of MIOI.

As shown above, better results are acquired by the improved method. In order to calculate the accuracy, RMSE of 10 pairs of corresponding points is employed, and it is defined as:

$$RMSE = \left\{ \frac{1}{N} \sum_{i=1}^N [(x_i - X_i)^2 + (y_i - Y_i)^2] \right\}^{\frac{1}{2}} \quad (4)$$

Where N = the number of corresponding points,  
 $x_i, y_i$  = point coordinates of reference image,  
 $X_i, Y_i$  = corresponding point coordinates of base image.  
 Table I compares the efficiency and accuracy of the above methods for the optical image and SAR image. We can see that our proposed method can greatly improve efficiency.

No	Reference coordinate (optical)	Original coordinate (SAR)	Registration coordinate (MIOI)	Registration coordinate (our method)
Experiment 1				
1	(65, -98)	(73, -98)	(28.505, -104.519)	(65.510, -96.499)
2	(197, -102)	(195, -109)	(148.250, -124.503)	(196.801, -103.404)
3	(221, -96)	(226, -103)	(179.002, -122.506)	(221.506, -96.250)
4	(350, -92)	(353, -103)	(307.750, -130.7505)	(348.750, -91.055)
5	(61, -117)	(70, -120)	(23.750, -125.500)	(61.500, -118.750)
6	(222, -123)	(226, -129)	(178.000, -147.250)	(222.250, -123.050)
7	(358, -123)	(362, -136)	(312.250, -160.500)	(357.815, -123.914)
8	(445, -122)	(450, -136)	(399.250, -170.750)	(444.359, -122.675)
9	(67, -149)	(69, -148)	(20.500, -155.500)	(67.679, -148.740)
10	(455, -76)	(460, -92)	(412.750, -127.500)	(454.257, -77.125)
RMSE <sub>1</sub> =1.2172 RMSE <sub>2</sub> =53.0914				
Experiment 2				
1	(67, -28)	(92.5, -31)	(74.500, -40.504)	(66.500, -28.000)
2	(137, -68)	(169.5, -81)	(159.500, -99.050)	(139.500, -69.510)
3	(359.5, -194.5)	(352.5, -198)	(368.500, -238.505)	(358.500, -192.495)
4	(467.5, -255.5)	(502.5, -292.5)	(440.500, -252.500)	(468.000, -254.500)
5	(352.5, 219)	(347.5, -219)	(364.070, -264.004)	(354.002, 218.500)
6	(436, -275)	(468, -308.5)	(406.100, -268.003)	(436.050, -273.500)
7	(449.5, -291)	(478.5, -328)	(420.502, -293.540)	(448.500, -290.500)
8	(379, -390.5)	(403.5, -423)	(353.508, -399.500)	(380.501, -389.499)
9	(260.5, -390.5)	(277, -421)	(222.005, -393.570)	(259.020, -390.001)

10	(296.5, -388.5)	(312.5, -421.5)	(262.500, -395.000)	(294.001, -388.020)
RMSE <sub>1</sub> =1.9261 RMSE <sub>2</sub> = 35.4894				
Experiment 3				
1	(121, -102)	(133.5, -102)	(135.500, -111.010)	(122.504, -102.490)
2	(391, -62)	(395, -81.5)	(394.500, -84.000)	(392.455, -64.504)
3	(198, -212)	(206, -209.5)	(207.000, -201.506)	(199.510, -211.505)
4	(221, -215)	(233, -212)	(234.500, -216.050)	(222.250, -215.500)
5	(200, -229)	(209.5, -236.5)	(213.504, -243.005)	(204.500, -228.105)
6	(221, -231)	(230, -241.5)	(238.500, -246.250)	(220.505, -231.510)
7	(28.5, -232)	(39, -222)	(45.005, -212.510)	(31.500, -232.025)
8	(9, -271)	(19.5, -255.5)	(24.500, -265.550)	(8.000, -269.525)
9	(342, -296.5)	(345.0, -305.5)	(351.500, -308.0500)	(343.005, -295.000)
10	(112, -437.5)	(109, -427.5)	(121.500, -425.500)	(112.755, -435.525)
RMSE <sub>1</sub> =1.6434 RMSE <sub>2</sub> = 18.6400				

Table I Comparison of the above methods. RMSE1 is result of our method. RMSE2 is result of MIOI

From the experimental results and quantitative analysis (Table I), some conclusions can be achieved:

- 1) The proposed method has better performance for the registration between optical and SAR images. Because of the changes in gray and effect of speckle noise, traditional methods are difficult to get satisfying result. Thanks to the local geometric information captured by voronoi diagram, the proposed method is robust to the two degradation factors.
- 2) Compared with other registration methods, the improved method is more stable. Voronoi diagram, which represents local geometric information of line intersections, is selected as the registration element. On the one hand, new inserted or removed points may change the local diagram, but don't affect the global stability; On the other hand, the change of local intersecting relationship of voronoi, will not disturb the global topology after affine transformation.
- 3) Compared with some methods with initial parameters, which will affect the result, the method introduced, could be more convenient.

#### 4. CONCLUSION

The proposed method is suitable to automatic registration of SAR and optical images with stable line features. It can greatly improve the stability and reliability of the registration algorithm by combing voronoi diagram with Graph Spectral Theory to determine the corresponding point sets. Our method can achieve

the automatic registration between optical and SAR images with high registration accuracy. However, the accuracy of line extraction affects the registration result. The point sets are based on line features. If the precision of line features isn't high, the accuracy of registration result will reduce, then, how to extract line features with high precision is our next step for improvement.

#### REFERENCES

- [1] AL Kesidis, N Papamarkos, 2000. A Window Based Inverse Hough Transform[J]. *Pattern Recognition*, 33:1 105-1 107.
- [2] G.L. Scott, H C. Longuet-Higgins, 1991. Algorithm for associating the features of two images [J]. *Proceedings of Royal Society of London*, B-244:21-26.
- [3] Jia Weijie, Zhang Jixian, and Yang Jinghui, 2009. Automatic registration of SAR and optics image based on multi-features on suburban areas, *Urban Remote Sensing Event, 2009 Joint* , pp.1-7.
- [4] Li H, Manjunath B S, and Mitra S K., 1993. "Optical-to-SAR registration using the active contour model" *IEEE Computer Society Conference on Signals, Systems and Computers*, pp. 568-572.
- [5] Li H, Manjunath B S, and Mitra S K. , 1995. A Contour-Based Approach to Multi-sensor Image Registration. *IEEE Transactions on Image Processing*, 4 (3), pp.320-334.
- [6] Lixia Shu, Tieniu Tan, Ming Tang, and Chunhong Pan, 2005. A Novel Registration Method for SAR and SPOT Images[C]. *IEEE International Conference on Image Processing ,ICIP 2005*, vol. 2. 13 -16.
- [7] L.S. Shapiro, J.M. Brady, 1992. Feature-based correspondence-An eigenvector approach [J]. *Image Vision Computer*, 10(5), pp.283-288.
- [8] MA Fischler, RC Bolles, 1987. *Random Sample Consensus: A Paradigm for Model Fitting with Applications to Image Analysis and Automated Cartography[M]*. San Francisco:Morgan Kaufmann PublishersInc,pp:726-740.
- [9] P. Dare, I. Dowman, 2001. "An improved model for automatic feature-based registration of SAR and SPOT image." *ISPRS Journal of photogrammetry & Remote Sensing*. pp: 13-28
- [10] Peng Fangyuan, 2009. "Automatic registration for optical and SAR remote sensing images based-on feature extraction," *Surveying and Mapping*, Vol. 32, pp. 257-262.
- [11] R. Touzi, A. Lopes, and P. Bousquet, 1988. A Statistical and Geometrical Edge Detector for SAR Images. *IEEE Trans.on Geoscience and Remote Sensing*. 26(6), pp.764-773.
- [12] Suri S., Reinartz, P., 2008. Application of generalized partial volume estimation for mutual information based registration of high resolution SAR and optical imagery, *Information Fusion, 2008 11th International Conference on*, pp.1-8
- [13] Wu Yingdan, Ming Yang, 2011. A Multi-sensor Remote Sensing Image Matching Method Based on SIFT Operator and CRA Similarity Measure, *Intelligence Science and Information Engineering (ISIE), 2011 International Conference on*, pp.115-118.
- [14] Xiaoxiang Wang and Jie Tian, 2005. Image registration based on maximization of gradient code mutual information. *Image Anal Stereol*, 24:1-7.
- [15] Zhang Dengrong, Yu Le, and Cai Zhigang, 2007. "A Region Feature Based Automatic Matching for Optical and SAR Images," *China University of Mining and Technology*, Vol. 36, pp. 843-847
- [16] Zhang ZhaoHui, Pan ChunHong, and Ma SongDe, 2004. "An automatic method of coarse registration between multi-source satellite images" *Intell. Sensors, Sensor Netw. and Info. Proc. Conf.*, vol.1 no.1, pp. 205-209.
- [17] Zhenhua Wang, Junping Zhang, Ye Zhang and Bin Zou, 2010. AUTOMATIC REGISTRATION OF SAR AND OPTICAL IMAGE BASED ON MULTI-FEATURES AND MULTI-CONSTRAINTS, *Geoscience and Remote Sensing Symposium (IGARSS), 2010 IEEE International* , pp. 1019-1022.